

Data-driven Control Against False Data Injection Attacks

Wenjie Liu^{a,c}, Lidong Li^b, Jian Sun^{a,c}, Fang Deng^{a,c}, Gang Wang^{a,c}, Jie Chen^{a,d}

^aState Key Lab of Autonomous Intelligent Unmanned Systems, School of Automation,
Beijing Institute of Technology, Beijing 100081, China

^bEngineering and Technology Institute, University of Groningen, 9747AG, The Netherlands

^cBeijing Institute of Technology Chongqing Innovation Center, Chongqing 401120, China

^dDepartment of Control Science and Engineering, Tongji University, Shanghai 201804, China

Abstract

The rise of cyber-security concerns has brought significant attention to the analysis and design of cyber-physical systems (CPSs). Among the various types of cyberattacks, denial-of-service (DoS) attacks and false data injection (FDI) attacks can be easily launched and have become prominent threats. While resilient control against DoS attacks has received substantial research efforts, countermeasures developed against FDI attacks have been relatively limited, particularly when explicit system models are not available. To address this gap, the present paper focuses on the design of data-driven controllers for unknown linear systems subject to FDI attacks on the actuators, utilizing input-state data. To this end, a general FDI attack model is presented, which imposes minimally constraints on the switching frequency of attack channels and the magnitude of attack matrices. A dynamic state feedback control law is designed based on offline and online input-state data, which adapts to the channel switching of FDI attacks. This is achieved by solving two data-based semi-definite programs (SDPs) on-the-fly to yield a tight approximation of the set of subsystems consistent with both offline clean data and online attack-corrupted data. It is shown that under mild conditions on the attack, the proposed SDPs are recursively feasible and controller achieves exponential stability. Numerical examples showcase its effectiveness in mitigating the impact of FDI attacks.

Key words: Data-driven control, switching false data injection attack, semi-definite program.

1 Introduction

Background and motivation: Although the widespread applications of cyber-physical systems (CPSs) in modern industrial processes offer superior efficiency, performance, and scalability [Lee \(2008\)](#); [Pasqualetti et al. \(2013\)](#), their cyber and networked aspects also introduce vulnerabilities that can be exploited through attacks, resulting in devastating damages, financial losses, and even harm to human lives [Luo et al. \(2023\)](#). Ac-

cording to Jerome Powell, Chairman of the Federal Reserve of the United States, cyberattacks have emerged as the foremost peril to the global financial system [Kotidis and Schreft \(2022\)](#). The COVID-19 pandemic and other recent crises have further amplified this risk, resulting in an upswing of cybercriminal activities, particularly ransomware attacks like the Kaseya VSA supply chain ransomware attack in 2021 [McMillan \(2021\)](#). Remarkably, cybercrime's economic toll is estimated at 1% of the world's GDP, equivalent to a staggering \$1,000 billion annually. This alarming metric emphasizes the exigent requirement for resilient cybersecurity measures and novel strategies to confront cyber threats.

Literature review: In general, cyberattacks can be categorized based on their target: disrupting the availability or compromising the integrity of transmitted information [Cárdenas et al. \(2008\)](#). The former, often manifested as communication interruptions caused by malicious jammers or routers, commonly employs denial-of-service (DoS) techniques [Hou et al. \(2022\)](#). Resilient control strategies have been developed since 2015, in e.g.

* The work was supported in part by the National Natural Science Foundation of China under Grants U23B2059, 62173034, 61925303, 62025301, 62088101, the China Scholarship Council under Grants 20206120009, 202206030127, and the Fundamental Research Funds for the Central Universities. (*Corresponding author: Gang Wang.*)

**This paper was not presented at any IFAC meeting.

Email addresses: liuwenjie@bit.edu.cn (Wenjie Liu), l.li@rug.nl (Lidong Li), sunjian@bit.edu.cn (Jian Sun), dengfang@bit.edu.cn (Fang Deng), gangwang@bit.edu.cn (Gang Wang), chenjie@bit.edu.cn (Jie Chen).

De Persis and Tesi (2015) to ensure acceptable performance even in the presence of such attacks. Noteworthy contributions in this area can be found in Feng and Tesi (2017); Liu et al. (2023a); Shi et al. (2022); Wakaiki et al. (2019) and their associated references.

On the other hand, the attackers aim to compromise data integrity by manipulating transmitted packets using false data injection (FDI) attacks. These attacks involve eavesdropping on authentic data and injecting false information, silently causing damage to the system performance without detection Cheng et al. (2019). Considerable efforts have been dedicated to designing detectors capable of raising alerts when anomalies are detected, ranging from model-based methods to data-driven methods, in e.g., Krishnan and Pasqualetti (2021); Mo et al. (2013); Pasqualetti et al. (2013); Wu et al. (2020). However, striking a balance between enhancing sensitivity to cyberattacks and minimizing false alarms during normal operation remains a challenge Bai et al. (2017). With the increasing sophistication and intelligence of attack strategies, the risk of undetectable attacks escalates, leading to devastating performance degradation. The recent focus has shifted from dealing with individual attacks to maintaining robustness in the presence of these attacks; see e.g., Anand and Teixeira (2022); Hashemi and Ruths (2022); Murguia et al. (2020); Wu et al. (2021).

Nonetheless, there are notable limitations with these existing results. Primarily, all the aforementioned studies require an explicit system model, which is difficult to obtain in real-world scenarios, see e.g. Coulson et al. (2019); De Persis and Tesi (2020); Li et al. (2023); Rotulo et al. (2022). Moreover, to pose constraints on the power of the attacker, it was assumed in Anand and Teixeira (2022); Hashemi and Ruths (2022); Murguia et al. (2020) that both the attacking gain matrix and the injected data are upper bounded. Although Wu et al. (2021) has relaxed this assumption by only constraining the attacking gain matrix, some historical false data should be collected *a priori*, making it less practical and appealing to confront more powerful attackers.

Contributions: This paper endeavors to stabilize unknown linear systems in the presence of FDI attacks on the controller-to-actuator channels, through the design of a time-varying state feedback controller from input-state data. A fundamental aspect of this problem revolves around the modeling of unknown FDI attacks in the context of data-driven control. In this regard, we refrain from making assumptions regarding the underlying attack strategy and instead consider a general attack model by only imposing constraints on the switching frequency of attack channels and bounding the attacking power. These considerations enable the reformulation of the FDI attacked system as a switched linear system, incorporating an unknown switching signal and unknown yet bounded subsystems. In this context, by exploring the data-based matrix ellipsoid

system representation method in Bisoffi et al. (2022), a data-based set encompassing all switching subsystems is constructed using offline clean data collected from the open-loop healthy system.

To accommodate scenarios where the attacker is too powerful such that stabilizing the set of systems consistent with offline data only becomes infeasible, we seek to merge online input-state observations to tighten the set approximation. Subsequently, an online state feedback controller is designed by stabilizing all systems contained in the reduced-size set obtained using both offline clean data and online attacked data. These two steps are accomplished by solving two data-based semi-definite programs (SDPs), which allows the controller to adapt to the channel switching of FDI attacks. Finally, we establish recursive feasibility for the developed data-based SDPs as well as exponential stability guarantees for the closed-loop data-driven control system under mild conditions on the attack.

In summary, the main contributions of the present paper are as follows.

- c1) A general FDI attack model is presented by constraining the switching frequency and the attack energy, allowing one to characterize the intensity of attacks;
- c2) A data-driven control method is developed, which returns a dynamic feedback controller by solving two data-based SDPs at each time; and,
- c3) Recursive feasibility of the two SDPs as well as exponential stability of the closed-loop attached system is established under mild conditions on the attack.

It is worth pointing out that there are several notable differences with respect to previous works Bisoffi et al. (2022); Wu et al. (2021). To begin, we modify the SDP in Bisoffi et al. (2022) by updating the data matrices at each time using online input-state data and adapt it to an LQR implementation. Due to these differences, stability of the system can be guaranteed only if recursive feasibility of the proposed SDP is ensured, whose proof deviates considerably from that of Bisoffi et al. (2022). In addition, although Wu et al. (2021) has modeled the attack-corrupted system as a switched system too, their focus is on how to design attack strategies to achieve maximum performance degradation. To our best knowledge, no previous work has considered resilient control against FDI attacks when the system model is unknown.

Notation: Denote the set of all real numbers, integers, non-negative, and positive integers by $\mathbb{R}, \mathbb{Z}, \mathbb{N}, \mathbb{N}_+$, respectively. For a matrix M , its rank is given by $\text{rank}(M)$; if it has full column (row) rank, its left (right) pseudo-inverse is denoted by M^\dagger . Given a vector $x \in \mathbb{R}^{n_x}$, let $\|x\|$ denote its Euclidean norm. The spectral norm of M is given by $\|M\|$. Moreover, $M \succ 0$ ($M \succeq 0$) means M is positive (semi-)definite, and $M \prec 0$ ($M \preceq 0$) means M is negative (semi-)definite. For matrices A, B and C with compatible dimensions, we abbreviate $ABC(AB)'$ to $AB \cdot C[\star]'$. Let $\underline{\lambda}_M$ ($\bar{\lambda}_M$) represent the minimum (max-

imum) singular value of a matrix M , and $\text{Tr}(M)$ denote the trace of the matrix M .

Given a signal $x : \mathbb{N} \rightarrow \mathbb{R}^{n_x}$ and any $T \in \mathbb{N}_+$, let $x_{[0,T-1]} := [x(0) \ x(1) \ \cdots \ x(T-1)]$ denote a stacked window of the signal x in the time interval $[0, T-1]$. The definition of persistence of excitation is adapted from [Willems et al. \(2005\)](#).

Definition 1.1 (Persistence of excitation) *Given any $L \in \mathbb{N}_+$, a signal $x_{[0,T-1]} \in \mathbb{R}^{n_x}$ with $T \geq (n_x + 1)L - 1$ is called persistently exciting of order L if $\text{rank}(H_L(x_{[0,T-1]})) = n_x L$ where $H_L(x_{[0,T-1]}) :=$*

$$\begin{bmatrix} x(0) & x(1) & \dots & x(T-L) \\ \vdots & \vdots & \ddots & \vdots \\ x(L-1) & x(L) & \dots & x(T-1) \end{bmatrix}.$$

2 Preliminaries and Problem Formulation

2.1 Healthy System

Consider the discrete-time linear state feedback system

$$x(t+1) = A_{\text{tr}}x(t) + B_{\text{tr}}u(t) \quad (1a)$$

$$u(t) = Kx(t) \quad (1b)$$

where $x(t) \in \mathbb{R}^{n_x}$ is the state, $u(t) \in \mathbb{R}^{n_u}$ is the control input, and $A_{\text{tr}} \in \mathbb{R}^{n_x \times n_x}$ and $B_{\text{tr}} \in \mathbb{R}^{n_x \times n_u}$ are fixed system matrices. The state feedback controller gain matrix K is to be designed. In this paper, we make the following standing assumptions.

Assumption 2.1 (Controllability) *The pair $(A_{\text{tr}}, B_{\text{tr}})$ in (1) is unknown but controllable.*

Assumption 2.2 (Offline data) *For some given integer $T \in \mathbb{N}_+$, input-state data $(u_{[0,T-1]}, x_{[0,T]})$ obtained from the open-loop healthy system (1a), are available, where the control input signal $u_{[0,T-1]}$ is persistently exciting of order $n_x + 1$.*

Assumption 2.2 is very common in the field of data-driven control, as seen in [Bisoffi et al. \(2022\)](#); [De Persis and Tesi \(2020\)](#); [Kang and You \(2023\)](#); [Rotulo et al. \(2022\)](#). To facilitate the subsequent design and analysis in this paper, we introduce the following data matrices associated with the signals $u_{[0,T-1]}$ and $x_{[0,T]}$:

$$U_0 = [u(0) \ \cdots \ u(T-1)], \quad X_0 = [x(0) \ \cdots \ x(T-1)] \quad (2a)$$

$$X_1 = [x(1) \ \cdots \ x(T)], \quad W_0 = [X_0' \ U_0']'. \quad (2b)$$

Under Assumption 2.2, it follows from ([Willems et al., 2005](#), Corollary 2) that the rank of W_0 satisfies $\text{rank}(W_0) = n_x + n_u$. This condition ensures that any length- T input-state trajectory of the open-loop system (1a) can be expressed as a linear combination of the columns of matrix W_0 ; that is, W_0 contains complete information about the system's dynamics in the sense that the system can be uniquely represented by using these offline data ([De Persis and Tesi, 2020](#), Theorem

1), i.e., $Z_{\text{tr}} := [A_{\text{tr}} \ B_{\text{tr}}]' = (X_1 W_0^\dagger)'$.

During online operation, we assume that the control input is transmitted over a vulnerable communication channel, e.g. a wireless channel, which is susceptible to FDI attacks. As a result, the integrity of the control input can be compromised, leading to adversarial changes in the system's dynamics (1a). In this context, our objective is to design a stabilizing controller in the form of (1b) to mitigate the impact of FDI attacks and ensure the closed-loop stability of the resultant FDI-corrupted system.

2.2 Switched FDI Attack

Before proceeding, we provide an overview of the FDI attack, which are aimed at manipulating the control signal and corrupting the dynamics to degrade system's performance or even cause instability. These attacks are typically modeled as additive inputs on the system state or sensor measurements [Pasqualetti et al. \(2013\)](#). Significant efforts have been devoted to designing strategies for launching FDI attacks to induce instability in the healthy system while evading detection [Fawzi et al. \(2014\)](#); [Wu et al. \(2020\)](#). In this paper, our focus is on designing a stabilizing controller for linear systems whose controller-to-actuator channels are subject to FDI attacks, rather than pursuing specific attacking strategies.

We consider a general FDI attack model as in [Wu et al. \(2020\)](#). In the offline phase, the attacker selects a set of attack matrices, one for each representing a possible combination of the controller-to-actuator channels. It further constructs an attack strategy determining the switching times between these combinations and the injected signal. During online operation, the attacker eavesdrops on the system state and determines the attack matrix according to its attack strategy. By multiplying the selected attack matrix with the current state, false data can be formed and injected into the corresponding controller-to-actuator channels. Different attack strategies and matrices could lead to different performances. We do not make any specific assumptions about the switching strategy of the attacker but simply constrain the magnitude of the attack matrices and the frequency of switching, which can be seen as limiting the capability and resources of the attacker.

To begin with, we introduce some assumptions regarding the attacker's behavior, which are general in the context of FDI attacks, e.g., [Murguia et al. \(2020\)](#); [Wu et al. \(2020\)](#). To distinguish the offline clean data $(x(t), u(t))$ in (1) from the attack-corrupted data, we denote the online corrupted state and input data as $(x_p(t), u_p(t))$. The following assumption is made.

Assumption 2.3 (FDI attack) *The FDI attack satisfies the following conditions.*

- i) *The attacker has access to the offline input-state data in Assumption 2.2. Based on the data, the attacker determines its attack strategy.*

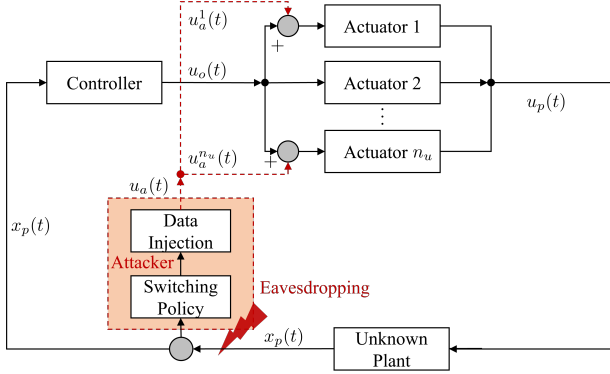


Fig. 1. System (5) under FDI attacks on actuators.

- ii) When an FDI attack occurs, the attacker eavesdrops on the plant-to-controller channel to obtain the current system state $x_p(t)$.
- iii) Based on $x_p(t)$ and the attack strategy, the attacker computes and injects the false data $u_a(t)$ into the state feedback control signal $u_o(t)$, so the actuators implement $u_p(t) = u_o(t) + u_a(t)$.

See Fig. 1 for a pictorial description of the considered setup. Under Assumption 2.3, the FDI attacked system is given by the following equations

$$x_p(t+1) = A_{\text{tr}}x_p(t) + B_{\text{tr}}u_p(t) \quad (3a)$$

$$u_p(t) = u_o(t) + u_a(t) \quad (3b)$$

$$u_o(t) = Kx_p(t). \quad (3c)$$

We consider a strong attacker which has access to and can compromise all controller-to-actuator channels at a time. Specifically, at each time t , the attacker may select a subset of these channels based on its strategy from the set $\mathcal{M} := \{1, 2, \dots, M\}$. Here, $M = \sum_{i=0}^{n_u} C_{n_u}^i$ represents the total number of attack choices, determined by the combination calculator C as $C_{n_u}^i = n_u!/(i!(n_u-i)!)$, totaling the number of combinations of channels. To model the switching of compromised channels by the attacker across time, we introduce a switching signal $\sigma(t) : \mathbb{N} \rightarrow \mathcal{M}$, which is a piece-wise constant function of time taking values in \mathcal{M} . The attacker utilizes different gain matrices selected from a prescribed set to corrupt the channels. At each time t , the false data are precisely obtained by multiplying the current state $x_p(t)$ with the matrix $D_a^{\sigma(t)} K_a^{\sigma(t)}$, where $D_a^{\sigma(t)}$ is the channel-selection matrix from $\{D_a^j \in \mathbb{R}^{n_u \times n_u} : j \in \mathcal{M}\}$ and $K_a^{\sigma(t)}$ is the attack matrix from $\{K_a^j \in \mathbb{R}^{n_u \times n_x} : j \in \mathcal{M}\}$ ¹.

Example 2.1 Let us consider a system as in (1) with $n_u = 3$ actuator channels, resulting in $M = \sum_{i=0}^3 C_3^i = 8$ different channel combinations $\emptyset, \{1\}, \{2\}, \{1, 2\}, \{1, 3\}, \{2, 3\}, \{1, 2, 3\}$, which are sequentially indexed by the elements in $\mathcal{M} = \{1, 2, 3, 4, 5, 6, 7, 8\}$. Suppose that

¹ Here, a unique attack matrix K_a^j for each channel-selection D_a^j is considered only for illustration of the key idea as well as ease of computing the total number of switching modes.

at time t the first and third channels (which therefore corresponds to the 6-th channel combination $\{1, 3\}$) are attacked, i.e., $\sigma(t) = 6$, and the associated channel-

$$\text{selection matrix } D_a^6 \text{ is given by } D_a^6 = \begin{bmatrix} 1 & 0 & 0 \\ 0 & 0 & 0 \\ 0 & 0 & 1 \end{bmatrix}.$$

2.3 System Remodeling and Problem Formulation

In the described setup above, the compromised system (3) under such FDI attacks can be equivalently reformulated as a switched linear system comprising M subsystems, operating under the switching signal $\sigma(t)$, i.e.,

$$x_p(t+1) = A_{\sigma(t)}x_p(t) + B_{\text{tr}}u_o(t) \quad (4a)$$

$$u_o(t) = Kx_p(t) \quad (4b)$$

where $A_{\sigma(t)} := A_{\text{tr}} + B_{\text{tr}}D_a^{\sigma(t)}K_a^{\sigma(t)} \in \{A_{\text{tr}} + B_{\text{tr}}D_a^jK_a^j : j \in \mathcal{M}\}$. We use t_s to denote the time when the s -th attack occurs, defined as $t_s := \min\{t > t_{s-1} : \sigma(t) \neq \sigma(t_{s-1})\}$ with $s \in \mathbb{N}_+$. Without loss of generality, we assume $t_0 = 0$. Suppose that the system is in mode j at time t_s , that is, $\sigma(t) = j$ for all $t \in [t_s, t_{s+1} - 1]$. In general, the attacker has limited resources. To reflect this fact, we make the following assumptions.

Assumption 2.4 (Switching frequency) For positive integers $t_1 \leq t_2$, let $N_\sigma(t_1, t_2)$ denote the number of discontinuities in signal σ over the interval $[t_1, t_2]$. There exist constants $\nu \geq 0$ and $\tau \geq 2$, referred to as the chatter bound and the average dwell-time, respectively, which satisfy $N_\sigma(t_1, t_2) \leq \nu + (t_2 - t_1)/\tau$.

Assumption 2.5 (Attacking power) There exists a constant $\phi > 0$ such that $\|D_a^jK_a^j\| \leq \phi$ holds for $j \in \mathcal{M}$.

Assumption 2.6 (Attacked system) The pairs (A_j, B_{tr}) for all $j \in \mathcal{M}$ are unknown to both the defender and attacker, but they are each assumed to be controllable.

These assumptions impose restrictions on the switching behavior, attacking power, and knowledge of the attacker, providing a framework for analyzing the cybersecurity of linear systems. In addition, note that $C_{n_u}^0 = 1$ indicates that no attacks occurs. This further means that Assumption 2.1 is implied in Assumption 2.6.

Define $\delta := \phi\|B_{\text{tr}}\|$. Under Assumptions 2.5 and 2.6, it can be easily seen that all switching subsystems $Z_j := [A_j \ B_{\text{tr}}]'$, $\forall j \in \mathcal{M}$, are contained in a set which are at most δ -far from the unknown true system $Z_{\text{tr}} := [A_{\text{tr}} \ B_{\text{tr}}]'$, defined by $\mathcal{B}^\delta := \{Z = [A \ B] : \|Z - Z_{\text{tr}}\| \leq \delta\}$. Building on this observation, a possible approach to stabilizing the unknown system (1) under the described FDI attacks is to design a static feedback controller K that stabilizes all subsystems (A_j, B_{tr}) , $\forall j \in \mathcal{M}$. Indeed, the previous work Wu et al. (2021) achieved this by assuming that the injected false data $u_a(t)$ can be collected offline and the matrices A_j can be identified by using a least-squares

algorithm. In practice however, obtaining access to the injection signal of the attacker is unrealistic, and finding a common static controller K to stabilize all subsystems is challenging or even impossible, especially when the matrices $\{(A_j, B_{tr})\}_{j \in \mathcal{M}}$ are not known.

To address this issue, we propose designing a dynamic feedback controller $u_o(t) = K(t)x_p(t)$ with the gain matrix $K(t)$ updated on-the-fly. Therefore, the switched system (4) becomes

$$x_p(t+1) = A_{\sigma(t)}x_p(t) + B_{tr}u_o(t) \quad (5a)$$

$$u_o(t) = K(t)x_p(t) \quad (5b)$$

where the switching signal $\sigma(t) : \mathbb{N} \rightarrow \mathcal{M}$ is dictated by the attacker and assumed unknown.

Building upon these preliminaries, we formally present the problem of interest as follows.

Problem 1 *Under Assumptions 2.2–2.6, design the time-varying state feedback controller $K(t)$ such that the switched system (5) achieves exponential stability.*

The focus of the remaining sections will be on addressing Problem 1.

3 Data-driven Control Against FDI

3.1 Data-driven Control Strategy

Learning a data-driven controller to achieve exponential stability of the unknown switched system (5) is challenging due to the presence of unknown subsystem matrices, switching signals, and switching times. The fresh idea we advocate here is to learn a controller $K(t)$ stabilizing a minimal subset of systems that contain the active switched subsystem $(A_{\sigma(t-1)}, B_{tr})$ and are consistent with the data at time t . To this aim, we first reformulate the set \mathcal{B}^δ using the offline data. In addition, we demonstrate that incorporating online data can help reduce the size of the set of feasible subsystems, increasing the possibility of finding a dynamic stabilizing controller. Finally, by solving two data-based SDPs at each time, we can construct a dynamic controller with guaranteed recursive feasibility for SDP as well as closed-loop system stability.

Recalling $Z_{tr} = [A_{tr} \ B_{tr}]' = (X_1 W_0^\dagger)'$, the set \mathcal{B}^δ can be equivalently converted into a quadratic matrix inequality (QMI) as follows

$$\mathcal{B}^\delta := \left\{ Z : Z'Z - Z'Z_{tr} - Z_{tr}'Z + \mathbf{C}^\delta \preceq 0 \right\} \quad (6)$$

where the constant

$$\mathbf{C}^\delta := Z_{tr}'Z_{tr} - \delta^2 I. \quad (7)$$

This set is essentially a matrix ball centered at the true system Z_{tr} with radius δ . It is clear that the larger the attacker's power δ is, the larger the volume of ball \mathcal{B}^δ is, and as a consequence, more "redundant" systems (those not belonging to the set of subsystems $\{(A_j, B_{tr})\}_{j \in \mathcal{M}}$) this ball contains. Although it is possible to search for

a static data-driven controller K stabilizing all the systems in \mathcal{B}^δ using Petersen's lemma [Bisoffi et al. \(2022\)](#) based on the offline data, this can be rather challenging especially when δ is large. In our proposal, we first leverage the online state-input data to obtain a tighter approximation of the set of feasible systems on top of \mathcal{B}^δ , and subsequently search for a dynamic controller stabilizing all systems in the reduced-size set.

During online operation, we assume that the initial conditions $u_p(0)$ and $x_p(0)$ are arbitrary. At time $t \in \mathbb{N}_+$, we have observed the online input-state data $(x_p(k-1), u_o(k-1), x_p(k))$ for all $k \leq t$. Nonetheless, due to the unknown switching signal $\sigma(\cdot)$, we do not know how exactly these data correspond to the M subsystems since they likely come from multiple subsystems. Therefore, it is difficult to directly employ all these online data to design a controller $K(t)$ to stabilize all subsystems. To bypass this challenge, we propose to combine only the most fresh data $(x_p(t-1), u_o(t-1), x_p(t))$ from the subsystem $(A_{\sigma(t-1)}, B_{tr})$ and the set of offline data from the healthy system (A_{tr}, B_{tr}) to design the controller $K(t)$ on the fly.

To this end, let us consider the switched system (5) at any time $t \in \mathbb{N}_+$, for which we have observed the online data $(x_p(t-1), u_o(t-1), x_p(t))$. The set of matrices $Z_t = [A_t \ B_t]'$ that can generate $(x_p(t-1), u_o(t-1), x_p(t))$ is given by

$$\mathcal{E}_t = \left\{ Z_t : \forall d(t-1) \in \mathbb{R}^{n_x} \text{ such that } d(t-1)d'(t-1) = 0, \right. \\ \left. x_p(t) = Z_t' \begin{bmatrix} x_p(t-1) \\ u_o(t-1) \end{bmatrix} + d(t-1) \right\}. \quad (8)$$

Since $d(t-1)d'(t-1) = 0$ in (8) can be implied by $d(t-1)d'(t-1) \preceq 0$, the result in ([van Waarde and Camlibel, 2021](#), (12)) has demonstrated its equivalence to the following QMI

$$[I \ d(t-1)] \begin{bmatrix} 0 & 0 \\ 0 & I \end{bmatrix} \begin{bmatrix} I \\ d'(t-1) \end{bmatrix} \preceq 0. \quad (9)$$

Moreover, we can rewrite $d(t-1) = x_p(t) - Z_t' \begin{bmatrix} x_p(t-1) \\ u_o(t-1) \end{bmatrix}$ and plug it into the QMI in (9), the set \mathcal{E}_t boils down to

$$\mathcal{E}_t = \left\{ Z_t : [I \ Z_t'] \begin{bmatrix} I & x_p(t) \\ 0 & -x_p(t-1) \\ 0 & -u_o(t-1) \end{bmatrix} \cdot \begin{bmatrix} 0 & 0 \\ 0 & I \end{bmatrix} [\star]' \preceq 0 \right\}.$$

Upon expanding the QMI and introducing

$$\mathbf{A}_t := \begin{bmatrix} x_p(t-1) \\ u_o(t-1) \end{bmatrix} \begin{bmatrix} x_p(t-1) \\ u_o(t-1) \end{bmatrix}' \quad (10a)$$

$$\mathbf{B}_t := - \begin{bmatrix} x_p(t-1) \\ u_o(t-1) \end{bmatrix} x_p'(t), \quad \mathbf{C}_t := x_p(t)x_p'(t) \quad (10b)$$

one can further re-express the set \mathcal{E}_t as follows

$$\mathcal{E}_t = \left\{ Z_t : Z_t' \mathbf{A}_t Z_t + Z_t' \mathbf{B}_t + \mathbf{B}_t' Z_t + \mathbf{C}_t \preceq 0 \right\} \quad (11)$$

which is a matrix ellipsoid too. It is evident that the active subsystem $[A_{\sigma(t-1)} \ B_{\text{tr}}]' \in \mathcal{E}_t$.

It is worth noting that the ellipsoid \mathcal{E}_t is degenerate and unbounded, even in the simplest case when $n_u = n_x = 1$ (Bisoffi et al., 2022, Lemma 2), due to the rank deficiency of matrix \mathbf{A}_t . Therefore, one cannot directly capitalize on Petersen's lemma Bisoffi et al. (2022) to design the controller $K(t)$.

Note from (6) that all subsystems are contained in \mathcal{B}^δ , which implies $Z_{\sigma(t-1)} = [A_{\sigma(t-1)} \ B_{\text{tr}}]' \in \mathcal{B}^\delta$ for all t . Combining this with (11), we conclude that

$$Z_{\sigma(t-1)} \in \mathcal{E}_t \cap \mathcal{B}^\delta, \quad \forall t \in \mathbb{N}_+. \quad (12)$$

Remark 3.1 (Z_t vs. $Z_{\sigma(t-1)}$) Symbols Z_t and $Z_{\sigma(t-1)}$ are used to refer to different types of matrices. Specifically, $Z_{\sigma(t-1)}$ represents the actual attacked system at time $t-1$. On the other hand, Z_t represents any matrices within the set \mathcal{E}_t , which include not only the actual attacked system matrices $Z_{\sigma(t-1)}$, but also other matrices consistent with the data $x_p(t)$, $x_p(t-1)$, $u_p(t-1)$.

The problem thus reduces to finding a controller $K(t)$ to stabilize all the systems in the set $\mathcal{E}_t \cap \mathcal{B}^\delta$ for all t . Nonetheless, it is difficult to analytically express the set $\mathcal{E}_t \cap \mathcal{B}^\delta$. In (Bisoffi et al., 2022, Section 4.4), a method for computing a set that over-approximates $\mathcal{E}_t \cap \mathcal{B}^\delta$ while minimizing the volume of the set is presented. Before moving on, we provide a brief review of this method.

Consider the following set

$$\mathcal{I}_t := \left\{ Z_t : Z_t' \bar{\mathbf{A}}_t Z_t + Z_t' \bar{\mathbf{B}}_t + \bar{\mathbf{B}}_t' Z_t + \bar{\mathbf{C}}_t \preceq 0 \right\}$$

with $\bar{\mathbf{A}}_t = \bar{\mathbf{A}}_t' \succ 0$ and $\bar{\mathbf{C}}_t = \bar{\mathbf{B}}_t' \bar{\mathbf{A}}_t^{-1} \bar{\mathbf{B}}_t - I$. This set can be equivalently rewritten as follows

$$\mathcal{I}_t = \left\{ Z_t : (Z_t + \bar{\mathbf{A}}_t^{-1} \bar{\mathbf{B}}_t)' \bar{\mathbf{A}}_t (Z_t + \bar{\mathbf{A}}_t^{-1} \bar{\mathbf{B}}_t) - I \preceq 0 \right\}$$

which represents a matrix ellipsoid centered at $-\bar{\mathbf{A}}_t^{-1} \bar{\mathbf{B}}_t$ with volume scaling with $-\log \det(\bar{\mathbf{A}}_t)$ as discussed in (Bisoffi et al., 2022, Section 4.4). Recalling the matrices \mathbf{C}^δ in (7) and $(\mathbf{A}_t, \mathbf{B}_t, \mathbf{C}_t)$ in (10), let $\bar{\mathbf{A}}_t^*$ and $\bar{\mathbf{B}}_t^*$ denote the optimal solutions of the following SDP problem (Bisoffi et al., 2022, (34))

$$\min_{\substack{\bar{\mathbf{A}}_t, \bar{\mathbf{B}}_t, \\ \tau_1 \geq 0, \tau_2 \geq 0}} -\log \det(\bar{\mathbf{A}}_t) \quad (13a)$$

$$\text{s.t. } \bar{\mathbf{A}}_t = \bar{\mathbf{A}}_t' \succ 0 \quad (13b)$$

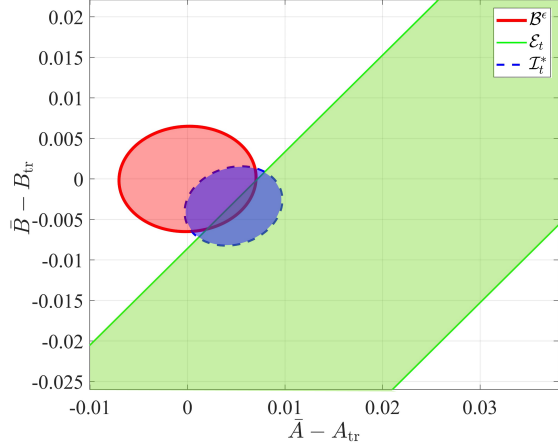


Fig. 2. Sets \mathcal{B}^δ (red solid circle), \mathcal{E}_t (green solid ellipsoid), and \mathcal{I}_t^* (blue dashed-line ellipsoid) for a first-order system.

$$\begin{bmatrix} -I & \bar{\mathbf{B}}_t' & \bar{\mathbf{B}}_t' \\ \bar{\mathbf{B}}_t & \bar{\mathbf{A}}_t & 0 \\ \bar{\mathbf{B}}_t & 0 & -\bar{\mathbf{A}}_t \end{bmatrix} - \tau_1 \begin{bmatrix} \mathbf{C}^\delta & -Z_{\text{tr}}' & 0 \\ -Z_{\text{tr}} & I & 0 \\ 0 & 0 & 0 \end{bmatrix} - \tau_2 \begin{bmatrix} \mathbf{C}_t & \mathbf{B}_t' & 0 \\ \mathbf{B}_t & \mathbf{A}_t & 0 \\ 0 & 0 & 0 \end{bmatrix} \preceq 0. \quad (13c)$$

Letting $\bar{\mathbf{C}}_t^* = \bar{\mathbf{B}}_t'^* \bar{\mathbf{A}}_t^{*-1} \bar{\mathbf{B}}_t^* - I$, the minimum-volume matrix ellipsoid containing the set $\mathcal{E}_t \cap \mathcal{B}^\delta$ is given by

$$\mathcal{I}_t^* = \left\{ Z_t : Z_t' \bar{\mathbf{A}}_t^* Z_t + Z_t' \bar{\mathbf{B}}_t^* + \bar{\mathbf{B}}_t'^* Z_t + \bar{\mathbf{C}}_t^* \preceq 0 \right\} \quad (14)$$

$$= \left\{ Z_t : (Z_t + \bar{\mathbf{A}}_t^{*-1} \bar{\mathbf{B}}_t^*)' \cdot \bar{\mathbf{A}}_t^* [\star]' - I \preceq 0 \right\}. \quad (15)$$

In addition, since the objective function $-\log \det(\bar{\mathbf{A}}_t)$ is a convex function, the SDP problem (13) with linear constraints is convex, and it can be solved efficiently using off-the-shelf convex optimization toolboxes.

Example 3.1 To provide a better understanding, the relationships between sets \mathcal{B}^δ , \mathcal{E}_t , and \mathcal{I}_t^* are illustrated in Fig. 2 using a first-order system with $A_{\text{tr}} = 1.021$, $B_{\text{tr}} = 0.041$, and $\delta = 0.025$.

From the figure, it is evident that if we can find a matrix $K(t)$ that stabilizes all the systems $Z_t = [A_t \ B_t]' \in \mathcal{I}_t^*$, then we can stabilize the system $(A_{\sigma(t-1)}, B) \in \mathcal{I}_t^*$ using $K(t)$. Finding a stabilizing controller for a set of systems characterized by a QMI has been studied in Bisoffi et al. (2022), in which such a controller $K(t)$ was obtained by resorting to Petersen's lemma. Building on this idea and inspired by the formulations for data-driven LQR and LQG control recently in De Persis and Tesi (2021); Liu et al. (2023b), we formulate the following SDP parameterized by the coefficient matrices defining the QMI (14) by balancing the system's performance and the robustness against FDI attacks

$$\begin{aligned}
& \min_{\gamma, P, Y, L, Q} \gamma \\
& \text{s.t.} \quad \begin{bmatrix} -\epsilon_1 P - \bar{\mathbf{C}}_t^* & 0 & \bar{\mathbf{B}}_t^* \\ 0 & -P & [P \ Y'] \\ \bar{\mathbf{B}}_t^* & [P \ Y']' & -\bar{\mathbf{A}}_t^* \end{bmatrix} \preceq 0 \quad (16a) \\
& P \succ 0 \quad (16b) \\
& \begin{bmatrix} L & Y \\ Y' & P \end{bmatrix} \succeq 0 \quad (16c) \\
& \begin{bmatrix} Q & I \\ I & P \end{bmatrix} \succeq 0 \quad (16d) \\
& \text{Tr}(P) + \text{Tr}(L) + \epsilon_2 \|Q\| \leq \gamma. \quad (16e)
\end{aligned}$$

Here, Constrains (16a) and (16b) guarantee that the resultant gain matrix $K(t)$ constructed by the optimal solutions is stabilizing; Constrains (16c)–(16e) are adapted from the robust data-driven LQR ensuring optimal performance of the consequent $K(t)$; and, the parameters $\epsilon_1 \in (0, 1)$ and $\epsilon_2 > 0$ are arbitrary, which balance the system's performance as well as feasibility of the SDP. Assume for now the SDP is feasible at each time t , and let $(\gamma^*(t), P^*(t), Y^*(t), L^*(t), Q^*(t))$ denote any optimal solution. The stabilizing controller $u_o(t) = K(t)x_p(t)$ for all systems in \mathcal{I}_t^* can be designed as follows

$$K(t) = Y^*(t)(P^*(t))^{-1}. \quad (17)$$

Based on (13)–(17), the proposed data-driven controller is summarized in Algorithm 1. However, successful implementation of Algorithm 1 hinges on the feasibility of SDP (16). Moreover, even if its feasibility is always ensured, it can be observed that at the switching time $t = t_s$, there is a mismatch between the mode of the controller and that of the system; that is, the active system is now $(A_{\sigma(t_s)}, B_{\text{tr}})$ while the computed controller $K(t)$ is designed for stabilizing the system $(A_{\sigma(t_{s-1})}, B_{\text{tr}})$. This mismatch may lead to the divergence of state trajectory if it happens frequently. To address problem 1 using Algorithm 1, we encounter two difficulties, which will be tackled in the following subsection, i.e., d1) how to ensure the feasibility of SDP (16) for all $t \in \mathbb{N}_+$? and, d2) under what conditions, can we stabilize the system (5)?

3.2 Theoretical Guarantees

In this subsection, we focus on answering the two questions in the previous subsection. The following result shows that if the attacking power δ is small, SDP (16) is feasible for all $t \in \mathbb{N}_+$ and the associated controller $K(t)$ is stabilizing.

Theorem 3.1 *Under Assumptions 2.1–2.6, let U_0, X_0 and X_1 be given in (2). Consider arbitrary initial conditions $x_p(0)$ and $u_o(0)$ for the system (5)*

Algorithm 1 Data-driven control against FDI.

- 1: **Offline:** Collect input-state data $(u_{[0, T-1]}, x_{[0, T]})$ and form matrices X_0, X_1, U_0, W_0 as in (2). Compute \mathcal{B}^δ as in (6).
 - 2: **Online:** Give initial conditions $x_p(0), u_o(0)$ and constants $\epsilon_1 \in (0, 1), \epsilon_2 > 0$.
 - 3: For $t = 1, 2, 3, \dots$, do
 - 1) Compute the matrix ellipsoid \mathcal{E}_t in (11) based on $u_o(t-1), x_p(t-1)$, and $x_p(t)$.
 - 2) Solve the SDP in (13) to obtain an over-approximation \mathcal{I}_t^* of the intersection $\mathcal{B}^\delta \cap \mathcal{E}_t$ as in (14).
 - 3) Solve the SDP in (16) for the set \mathcal{I}_t^* and denote the solution as $(\gamma^*(t), P^*(t), Y^*(t), L^*(t), Q^*(t))$.
 - 4) Compute the control input $u_o(t) = K(t)x_p(t)$, where $K(t) = Y^*(t)(P^*(t))^{-1}$ is given in (17).
 - 5) Set $t = t + 1$ and go back to 1).
-

with Algorithm 1. There exist constants $\bar{\delta} > 0$ and $\epsilon_1 \in (0, 1)$ such that for all $\delta \in [0, \bar{\delta})$ and $\epsilon_1 \in (\epsilon_1, 1)$, SDP (16) is feasible for any $t \in \mathbb{N}_+$ with an optimal solution $(\gamma^*(t), P^*(t), Y^*(t), L^*(t), Q^*(t))$. Let $K(t) = Y^*(t)(P^*(t))^{-1}$. Then the following statements hold true:

- s1) Let $j = \sigma(t_s)$ denote the active subsystem for all $t \in [t_s, t_{s+1} - 1]$. Then the controller $K(t)$ stabilizes the subsystem (A_j, B_{tr}) .
- s2) There exists a constant $\kappa > 0$ such that $\|K(t)\| \leq \kappa$ for all $t \in \mathbb{N}_+$.

PROOF. Consider any $s \in \mathbb{N}$ and $t \in [t_s + 1, t_{s+1}]$, and let $j = \sigma(t_s)$ denote the active subsystem $Z_{\sigma(t-1)} = Z_j = [A_j \ B_{\text{tr}}]'$. It is clear from the previous subsection that $Z_j \in \mathcal{E}_t \cap \mathcal{B}^\delta \subseteq \mathcal{I}_t^*$. The key idea of the proof is to construct a candidate solution for SDP (16). To this end, we explore the data-driven LQR formulation of subsystem (A_j, B_{tr}) by showing that, under certain conditions on the attacking power δ and the parameter ϵ_1 , a candidate solution of SDP (16) can be constructed from the LQR solution. This establishes the feasibility of SDP (16), and statements s1) and s2) can be proved.

i) *Proof of Feasibility of SDP (16)*

According to (15), although the subsystem $Z_j = [A_j \ B_{\text{tr}}]'$ is active for all $t \in [t_s + 1, t_{s+1}]$, the matrix Z_j is generally not the center of the ellipsoid \mathcal{I}_t^* . This renders the feasibility and stability analysis rather complicated. To overcome this difficulty, we construct a matrix ball \mathcal{B}^{δ_j} centered at Z_j with some radius δ_j such that $\mathcal{I}_t^* \subseteq \mathcal{B}^{\delta_j}$. Hence, to prove the feasibility of SDP (16) for \mathcal{I}_t^* , it suffices to prove that for the ball \mathcal{B}^{δ_j} . Building on this observation, we start by defining \mathcal{B}^{δ_j} , and subsequently review the data-driven LQR formulation, based on which we construct a candidate solution of SDP (16) for set \mathcal{B}^{δ_j} .

Consider the ball centered at Z_j with radius δ_j as follows

$$\mathcal{B}^{\delta_j} := \left\{ Z : Z'Z - Z'Z_j - Z_j'Z + \mathbf{C}^{\delta_j} \preceq 0 \right\} \quad (18)$$

where $\mathbf{C}^{\delta_j} := Z_j' Z_j - \delta_j^2 I$. Since \mathcal{I}_t^* is bounded, there exists some constant $\bar{\delta}_j \in (0, \delta]$ such that for all $\delta_j \in (\bar{\delta}_j, \delta]$, it holds that $\cup_{t=t_s+1}^{t=t_s+1} \mathcal{I}_t^* \subseteq \mathcal{B}^{\delta_j}$ for any $s \in \mathbb{N}$. This indicates that if SDP (16) is feasible for set \mathcal{B}^{δ_j} , it is feasible for \mathcal{I}_t^* for all $t \in [t_s + 1, t_{s+1}]$ too.

By replacing the matrices $\bar{\mathbf{A}}_t^*$, $\bar{\mathbf{B}}_t^*$ and $\bar{\mathbf{C}}_t^*$ in (16) with I , $-Z_j$, and \mathbf{C}^{δ_j} , respectively, we formulate the following SDP for set \mathcal{B}^{δ_j} and continue to derive conditions for its feasibility

$$\begin{aligned} & \min_{\gamma, P, Y, L, Q} \gamma \\ & \text{s.t.} \begin{bmatrix} -\epsilon_1 P - \mathbf{C}^{\delta_j} & 0 & -Z_j' \\ 0 & -P & [P \ Y'] \\ -Z_j & [P \ Y']' & -I \end{bmatrix} \preceq 0 \quad (19a) \\ & P \succ 0 \quad (19b) \\ & \begin{bmatrix} L & Y \\ Y' & P \end{bmatrix} \succeq 0 \quad (19c) \\ & \begin{bmatrix} Q & I \\ I & P \end{bmatrix} \succeq 0 \quad (19d) \\ & \text{Tr}(P) + \text{Tr}(L) + \epsilon_2 \|Q\| \leq \gamma. \quad (19e) \end{aligned}$$

Before proceeding, we recall Petersen's lemma in Bisoffi et al. (2022), which plays an important role in the rest of the proof. Since \mathcal{B}^{δ_j} is bounded, it has been demonstrated in (Bisoffi et al., 2022, Theorem 1) that the feasibility problem

$$\begin{aligned} & \text{find } Y, P = P' \succ 0 \quad (20) \\ & \text{s.t. } [A \ B] \begin{bmatrix} P \\ Y \end{bmatrix} \cdot P^{-1}[\star]' - P \prec 0, \quad \forall [A \ B]' \in \mathcal{B}^{\delta_j} \end{aligned}$$

is equivalent to that of

$$\begin{aligned} & \text{find } Y, P = P' \succ 0, \lambda > 0 \quad (21) \\ & \text{s.t.} \begin{bmatrix} -\lambda P - \mathbf{C}^{\delta_j} & 0 & -Z_j' \\ 0 & -\lambda P & \lambda [P \ Y'] \\ -Z_j & \lambda [P \ Y']' & -I \end{bmatrix} \prec 0. \end{aligned}$$

To show the feasibility SDP (19), we begin by considering the set \mathcal{B}^{δ_j} with $\delta_j = 0$. In this case, the matrix \mathbf{C}^{δ_j} reduces to $\mathbf{C}^{\delta_j} = \mathbf{C}^0 = Z_j' Z_j$. Recall from Assumption 2.6 that the system $[A_j \ B_{\text{tr}}]$ is controllable. Thus, there is a unique LQR controller. Building on (De Persis and Tesi, 2021, (9)), the LQR controller gain for system $[A_j \ B_{\text{tr}}]$ can be found by using the optimal solution of the following SDP

$$(\tilde{\gamma}_j, \tilde{P}_j, \tilde{Y}_j, \tilde{L}_j) := \arg \min_{\gamma, P, Y, L} \gamma$$

$$\text{s.t. } [A_j \ B_{\text{tr}}] \begin{bmatrix} P \\ Y \end{bmatrix} \cdot P^{-1}[\star]' - P + I \preceq 0 \quad (22a)$$

$$P \succeq I \quad (22b)$$

$$\begin{bmatrix} L & Y \\ Y' & P \end{bmatrix} \succeq 0 \quad (22c)$$

$$\text{Tr}(P) + \text{Tr}(L) \leq \gamma. \quad (22d)$$

Moreover, at the optimum, constraint (22a) becomes

$$[A_j \ B_{\text{tr}}] \begin{bmatrix} \tilde{P}_j \\ \tilde{Y}_j \end{bmatrix} \cdot \tilde{P}_j^{-1}[\star]' - \tilde{P}_j \preceq -I \prec 0 \quad (23)$$

which implies (20) with $\delta_j = 0$. Since (20) is equivalent to (21), there exist some constants $\lambda_j > 0$ and $\rho_j > 0$ such that

$$\begin{bmatrix} -\lambda_j \tilde{P}_j - Z_j' Z_j & 0 & -Z_j' \\ 0 & -\lambda_j \tilde{P}_j & \lambda_j [\tilde{P}_j \ \tilde{Y}_j'] \\ -Z_j & \lambda_j [\tilde{P}_j \ \tilde{Y}_j']' & -I \end{bmatrix} \preceq -\rho_j I. \quad (24)$$

Based on this inequality, we consider $\delta_j \geq 0$ and derive conditions on ϵ_1 and δ_j such that a candidate solution of SDP (19) can be constructed using $(\tilde{\gamma}_j, \tilde{P}_j, \tilde{Y}_j, \tilde{L}_j)$. The remaining proof is divided into two parts depending on whether $\lambda_j \in (0, 1)$ or $\lambda_j \geq 1$.

Case 1: $\lambda_j \in (0, 1)$.

When $\lambda_j \in (0, 1)$, substituting (24) into constraint (19a) yields

$$\begin{aligned} & \begin{bmatrix} -\lambda_j \tilde{P}_j - Z_j' Z_j & 0 & -Z_j' \\ 0 & -\lambda_j \tilde{P}_j & \lambda_j [\tilde{P}_j \ \tilde{Y}_j'] \\ -Z_j & \lambda_j [\tilde{P}_j \ \tilde{Y}_j']' & -I \end{bmatrix} \\ & + \begin{bmatrix} (1 - \epsilon_1) \lambda_j \tilde{P}_j + \delta_j^2 I & 0 & 0 \\ 0 & 0 & 0 \\ 0 & 0 & 0 \end{bmatrix} \\ & \preceq -\rho_j I + \begin{bmatrix} (1 - \epsilon_1) \lambda_j \tilde{P}_j + \delta_j^2 I & 0 & 0 \\ 0 & 0 & 0 \\ 0 & 0 & 0 \end{bmatrix}. \quad (25) \end{aligned}$$

Hence, if $\epsilon_1 \in (0, 1)$ is chosen large enough such that $\rho_j I - (1 - \epsilon_1) \lambda_j \tilde{P}_j \succeq 0$, then for all $\delta_j \in [0, \tilde{\delta}_j]$ with $\tilde{\delta}_j \leq \sqrt{\|\rho_j I - (1 - \epsilon_1) \lambda_j \tilde{P}_j\|}$, the right-hand side of inequality (25) is negative semi-definite. This ensures that constraint (19a) is satisfied. If we can construct γ , L , and Q satisfying constraints (19b)–(19e), the feasibility of SDP (19) is proved.

$$\begin{bmatrix} -\epsilon_1 \mu_j^{\lambda_j} \tilde{P}_j^{\lambda_j} - \bar{\mathbf{C}}^{\delta_j} & 0 & -Z_j' \\ 0 & -\mu_j^{\lambda_j} \tilde{P}_j^{\lambda_j} & \mu_j^{\lambda_j} [\tilde{P}_j^{\lambda_j} \tilde{Y}_j^{\lambda_j}]' \\ -Z_j & \mu_j^{\lambda_j} [\tilde{P}_j^{\lambda_j} \tilde{Y}_j^{\lambda_j}]' & -I \end{bmatrix} \preceq \begin{bmatrix} -\mu_j^{\lambda_j} \rho_j I + (\mu_j^{\lambda_j} (1 - \epsilon_1) \tilde{P}_j^{\lambda_j} - (1 - \mu_j^{\lambda_j}) Z_j' Z_j + \delta_j^2 I) & 0 & (\mu_j^{\lambda_j} - 1) Z_j' \\ 0 & -\mu_j^{\lambda_j} \rho_j I & 0 \\ (\mu_j^{\lambda_j} - 1) Z_j & 0 & -\mu_j^{\lambda_j} \rho_j I + (\mu_j^{\lambda_j} - 1) I \end{bmatrix} \quad (30)$$

By letting $\tilde{Q}_j := (\lambda_j \tilde{P}_j)^{-1}$ and $\hat{\gamma}_j := \tilde{\gamma}_j + \|\tilde{P}_j^{-1}\| \epsilon_2 / \lambda_j$, it is evident that constraints (19b)–(19e) are automatically satisfied. Therefore, $(\hat{\gamma}_j, \lambda_j \tilde{P}_j, \lambda_j \tilde{Y}_j, \lambda_j \tilde{L}_j, \tilde{Q}_j)$ is a candidate solution of SDP (19) and one has from $\mathcal{I}_t^* \subseteq \mathcal{B}^{\delta_j}$ that SDP (16) is feasible for set \mathcal{I}_t^* .

Case 2: $\lambda_j \geq 1$.

When $\lambda_j \geq 1$, letting $\tilde{P}_j^{\lambda_j} := \lambda_j \tilde{P}_j$, $\tilde{Y}_j^{\lambda_j} := \lambda_j \tilde{Y}_j$, $\tilde{L}_j^{\lambda_j} := \lambda_j \tilde{L}_j$ and $\tilde{\gamma}_j^{\lambda_j} := \lambda_j \tilde{\gamma}_j$, in the following, we first show that $(\tilde{P}_j^{\lambda_j}, \tilde{Y}_j^{\lambda_j}, \tilde{L}_j^{\lambda_j}, \tilde{\gamma}_j^{\lambda_j})$ is a candidate solution of problem (22) and then use these variables to construct a candidate solution for SDP (19).

Since $\lambda_j \geq 1$, constraints (22b)–(22d) are automatically satisfied. Multiplying both sides of (23) with λ_j , one gets that

$$\lambda_j [A_j \ B_{\text{tr}}] \begin{bmatrix} \tilde{P}_j \\ \tilde{Y}_j \end{bmatrix} \cdot \tilde{P}_j^{-1} [\star]' - \lambda_j \tilde{P}_j \preceq -\lambda_j I \preceq -I$$

which implies that (22a) is satisfied. Hence $(\tilde{P}_j^{\lambda_j}, \tilde{Y}_j^{\lambda_j}, \tilde{L}_j^{\lambda_j}, \tilde{\gamma}_j^{\lambda_j})$ is a candidate solution to SDP (22).

We now consider $(\tilde{P}_j^{\lambda_j}, \tilde{Y}_j^{\lambda_j}, \tilde{L}_j^{\lambda_j}, \tilde{\gamma}_j^{\lambda_j})$ and show that there exists some $\mu_j^{\lambda_j} \in (0, 1)$, such that constraint (19a) is satisfied at $(\mu_j^{\lambda_j} \tilde{P}_j^{\lambda_j}, \mu_j^{\lambda_j} \tilde{Y}_j^{\lambda_j})$ under some conditions on ϵ_1 and δ_j . Noting that inequality (24) becomes

$$\begin{bmatrix} -\tilde{P}_j^{\lambda_j} - Z_j' Z_j & 0 & -Z_j' \\ 0 & -\tilde{P}_j^{\lambda_j} & [\tilde{P}_j^{\lambda_j} \tilde{Y}_j^{\lambda_j}]' \\ -Z_j & [\tilde{P}_j^{\lambda_j} \tilde{Y}_j^{\lambda_j}]' & -I \end{bmatrix} \preceq -\rho_j I. \quad (26)$$

Multiplying both sides of inequality (26) by $\mu_j^{\lambda_j}$ and substituting it into constraint (19a) yields (30), which is presented at the top of the next page. Since $\mu_j^{\lambda_j} \in (0, 1)$, based on Schur complement lemma, if

$$\begin{aligned} & -\mu_j^{\lambda_j} \rho_j I + \mu_j^{\lambda_j} (1 - \epsilon_1) \tilde{P}_j^{\lambda_j} + \delta_j^2 I \\ & - (1 - \mu_j^{\lambda_j}) Z_j' Z_j - \frac{(1 - \mu_j^{\lambda_j})^2}{-\mu_j^{\lambda_j} \rho_j + \mu_j^{\lambda_j} - 1} Z_j' Z_j \\ & \prec -\mu_j^{\lambda_j} \rho_j I + \mu_j^{\lambda_j} (1 - \epsilon_1) \tilde{P}_j^{\lambda_j} + \delta_j^2 I \preceq 0 \end{aligned} \quad (31)$$

then constraint (19a) is satisfied. Therefore, if $\epsilon_1 \in (0, 1)$ is chosen rendering $\rho_j I - (1 - \epsilon_1) \tilde{P}_j^{\lambda_j} \prec 0$, then for $\delta_j \in [0, \tilde{\delta}_j]$ with $\tilde{\delta}_j \leq \sqrt{\mu_j \|\rho_j I - (1 - \epsilon_1) \tilde{P}_j^{\lambda_j}\|}$, inequality (31) is satisfied. Moreover, since $\tilde{\delta}_j \leq \delta$, we can find a positive constant $\bar{\delta} > 0$ such that inequality (31) is satisfied and consequently (30) is non-positive for all $\delta \in [0, \bar{\delta}]$. This inequality guarantees the satisfaction of constraint (16a).

Moreover, letting $\hat{\gamma}_j^{\lambda_j} := \tilde{\gamma}_j^{\lambda_j} + \epsilon_2 \|\tilde{Q}_j^{\lambda_j}\|$ and $\tilde{Q}_j^{\lambda_j} := (\tilde{P}_j^{\lambda_j} \mu_j^{\lambda_j})^{-1}$, similar to the proof for the case $\lambda_j \in (0, 1)$, constraints (19b)–(19e) are automatically satisfied. Hence, $(\hat{\gamma}_j^{\lambda_j}, \mu_j^{\lambda_j} \tilde{P}_j^{\lambda_j}, \mu_j^{\lambda_j} \tilde{Y}_j^{\lambda_j}, \mu_j^{\lambda_j} \tilde{L}_j^{\lambda_j}, \tilde{Q}_j^{\lambda_j})$ is a solution to SDP (19), indicating that for all $\delta \in [0, \bar{\delta}]$, SDP (16) is feasible.

So far, we have established the feasibility of SDP (16). Let $(\gamma^*(t), P^*(t), Y^*(t), L^*(t), Q^*(t))$ be an optimal solution of (16) at time t and $K(t) = Y^*(t)(P^*(t))^{-1}$. In the sequel, we prove the statements s1) and s2).

ii) *Proof of statements s1) and s2).*

Since $Z_j = [A_j \ B_{\text{tr}}]' \in \mathcal{I}_t^*, \forall t \in [t_s + 1, t_{s+1}]$, according to (Bisoffi et al., 2022, Theorem 1), the feasibility of (16) implies the following inequality

$$[A_j + B_{\text{tr}} K(t)] \cdot P^*(t) [\star]' - P^*(t) \preceq (\epsilon_1 - 1) P^*(t). \quad (32)$$

This further indicates that $K(t)$ stabilizes the subsystem (A_j, B_{tr}) for all $t \in [t_s + 1, t_{s+1}]$, which proves statement s1).

To show statement s2), we recall that \tilde{P}_j and \tilde{K}_j correspond to the unique LQR solutions for the subsystem (A_j, B_{tr}) . Since $\gamma^*(t) \leq \hat{\gamma}_j$ if $\lambda_j \in (0, 1)$ with $\hat{\gamma}_j = \lambda_j \tilde{\gamma}_j + \epsilon_2 \|\tilde{P}_j^{-1}\| / \lambda_j$ (or $\gamma^*(t) \leq \hat{\gamma}_j^{\lambda_j}$ if $\lambda_j \geq 1$ with $\hat{\gamma}_j^{\lambda_j} = \mu_{t_j}^{\lambda_j} \tilde{\gamma}_j^{\lambda_j} + \epsilon_2 \|(\tilde{P}_j^{\lambda_j})^{-1}\| / \mu_{t_j}^{\lambda_j}$), it follows that $\|(P^*(t))^{-1}\| \leq \hat{\gamma}_j / \epsilon_2$ if $\lambda_j \in (0, 1)$ (or $\|(P^*(t))^{-1}\| \leq \hat{\gamma}_j^{\lambda_j} / \epsilon_2$ if $\lambda_j \geq 1$). Hence, $P^*(t) \succeq \epsilon_2 / \hat{\gamma}_j I$ if $\lambda_j \in (0, 1)$ (or $P^*(t) \succeq \epsilon_2 / \hat{\gamma}_j^{\lambda_j} I$ if $\lambda_j \geq 1$). It can be deduced from (16c)–(16d) that

$$\begin{aligned} \|K(t)\| & \leq \sqrt{\text{Tr}(K(t) I K'(t))} \\ & \leq \sqrt{\text{Tr}(K(t) P^*(t) K'(t)) \max\{\hat{\gamma}_j, \hat{\gamma}_j^{\lambda_j}\} / \epsilon_2} \\ & \leq \sqrt{\text{Tr}(L^*(t)) \max\{\hat{\gamma}_j, \hat{\gamma}_j^{\lambda_j}\} / \epsilon_2} \end{aligned}$$

$$\leq \sqrt{\max\{\hat{\gamma}_j, \hat{\gamma}_j^{\lambda_j}\}^2 / \epsilon_2}.$$

Consequently, statement s2) can be proven by setting

$$\kappa := \max_{j \in \mathcal{M}} \sqrt{\max\{\hat{\gamma}_j, \hat{\gamma}_j^{\lambda_j}\}^2 / \epsilon_2}.$$

Remark 3.2 (Complexity) *The proposed controller requires computing SDPs (13) and (16) at each time. According to (Sznaier, 2020, Section G), the complexity of solving SDP (13) is roughly $\mathcal{O}((n_x + n_u)^3(2n_x + n_u)^3)$ and that of solving SDP (16) is roughly $\mathcal{O}(n_x^3(n_x + n_u)^3)$. One can further consolidate these two SDPs into a single SDP as follows*

$$\min_{\substack{\gamma, \beta, \tau_1, \tau_2, \\ P, Y, L, Q}} \gamma \quad (33a)$$

$$\text{s.t.} \quad \begin{bmatrix} P - \beta I & 0 & 0 & 0 \\ 0 & -P - Y' & 0 & 0 \\ 0 & -Y & 0 & Y \\ 0 & 0 & Y' & P \end{bmatrix} - \tau_1 \begin{bmatrix} -\mathbf{C}_t - \mathbf{B}'_t & 0 \\ -\mathbf{B}_t - \mathbf{A}_t & 0 \\ 0 & 0 & 0 \end{bmatrix}$$

$$- \tau_2 \begin{bmatrix} -\mathbf{C}^\delta & -Z'_{\text{tr}} & 0 \\ 0 & -I & 0 \\ 0 & 0 & 0 \end{bmatrix} \succeq 0 \quad (33b)$$

$$\beta > 0, \quad \tau_1 \geq 0, \quad \tau_2 \geq 0, \quad P \succ 0 \quad (33c)$$

$$\begin{bmatrix} L & Y \\ Y' & P \end{bmatrix} \succeq 0 \quad (33d)$$

$$\begin{bmatrix} Q & I \\ I & P \end{bmatrix} \succeq 0 \quad (33e)$$

$$\text{Tr}(P) + \text{Tr}(L) + \epsilon \|Q\| \leq \gamma. \quad (33f)$$

In this manner, the computational complexity reduces to $\mathcal{O}(n_x^3(n_x + n_u)^3)$, which is smaller than $\mathcal{O}(n_x^3(n_x(n_u + 1) + n_u)^3)$ in Rotulo et al. (2022).

Remark 3.3 (Noisy data) *The proposed method can be directly extended to handle noisy data. Instead of considering the ideal system (1), we consider a system with noise, i.e., $x(t+1) = Ax(t) + Bu(t) + w(t)$, where the process noise $w(t)$ satisfies $\|w(t)\| \leq \bar{w}$ for all $t \in \mathbb{N}$. In this setting, the value of δ is affected by both the attack matrix and the noise level \bar{w} . During the online step, the matrix \mathbf{C}_t in (10b) can be replaced by $\mathbf{C}_t = x_p(t)x_p'(t) - \bar{w}^2 I$ to compensate for noise.*

Thus far, we have established the feasibility for SDP (16) provided that certain conditions on the attacking power δ and the parameter ϵ_1 are met. In addition, matrix $K(t)$ defined in (17) stabilizes the subsystem $(A_{\sigma(t_s)}, B_{\text{tr}})$ for $t \in [t_s + 1, t_{s+1}]$. However, observing at time $t = t_{s+1}$ that the dynamics switches to $(A_{\sigma(t_{s+1})}, B_{\text{tr}})$ while the matrix $K(t)$ is designed to stabilize $(A_{\sigma(t_s)}, B_{\text{tr}})$. Consequently, there is a mismatch between the controller gain $K(t)$ and the activated mode $\sigma(t_{s+1})$, which may lead

to divergence of the state. Hence, in the following, conditions on the attacker's switching frequency is derived to ensure the stability of system (5).

Remark 3.4 (Parameters ϵ_1 and ϵ_2) *It has been shown in the proof of Theorem 3.1 that a larger ϵ_1 enables the feasibility of SDP (16) under a larger attack energy bound δ . The largest bound is achieved when $\epsilon_1 = 1$. In this case, constraint (16a) should be modified into a strict form, i.e., replacing \preceq with \prec . On the other hand, inequalities (32) and (34) in the proof of Theorem 3.2 imply that a smaller ϵ_1 and a larger $P^*(t)$ provides a faster convergence rate, which leads to better system's performance as we illustrate through numerical examples in the ensuing section. The parameter ϵ_1 trades off between the feasibility of SDP (16) and the system's performance. Furthermore, as discussed before, system's performance benefits from a larger $P^*(t)$, according to (16d) and (16e), which can be realized by choosing a larger ϵ_2 .*

Theorem 3.2 *Under Assumptions 2.2–2.6, let U_0, X_0 , and X_1 be given in (2). There exists constants $\bar{\delta} > 0$, $\bar{\tau} \geq 2$ such that for all $\delta \in [0, \bar{\delta})$ and $\tau > \bar{\tau}$, the system (5) with Algorithm 1 is exponentially stable, for arbitrary initial conditions $x_p(0)$ and $u_o(0)$.*

PROOF. Consider the system (5) in any switching interval $[t_s, t_{s+1} - 1]$ with Algorithm 1. Let $j \in \mathcal{M}$ denote the subsystem selected by $\sigma(t_s)$, i.e., $j = \sigma(t)$ for all $t \in [t_s, t_{s+1} - 1]$. First, we demonstrate the convergence of the state for all $t \in [t_s + 2, t_{s+1}]$ and any $s \in \mathbb{N}$. By bounding the distance between $x(t_s + 1)$ and $x(t_s)$, we can achieve stability under mild conditions on the switching frequency and the attacking power.

According to statement s1) of Theorem 3.1, it follows that for all $t \in [t_s + 1, t_{s+1}]$, SDP (16) is feasible with an optimal solution $(\gamma^*(t), P^*(t), Y^*(t), L^*(t), Q^*(t))$, and $K(t) = Y^*(t)(P^*(t))^{-1}$ stabilizes (A_j, B_{tr}) . Therefore, there exist $P_j \succ 0$ and $\alpha_j \in (0, 1)$ such that

$$(A_j + B_{\text{tr}}K(t))'P_j(A_j + B_{\text{tr}}K(t)) - P_j \preceq -\alpha_j I \quad (34)$$

holds for all $t \in [t_s + 1, t_{s+1}]$.

We construct a Lyapunov function $V_j(t) = x_p'(t)P_jx_p(t)$, which satisfies the inequalities

$$\lambda_P \|x_p(t)\|^2 \leq V_j(t) \leq \bar{\lambda}_P \|x_p(t)\|^2 \quad (35)$$

where $\lambda_P := \min_{j \in \mathcal{M}} \lambda_{P_j}$ and $\bar{\lambda}_P := \max_{j \in \mathcal{M}} \bar{\lambda}_{P_j}$.

For $t \in [t_s + 1, t_{s+1} - 1]$, it can be deduced that $V_j(t + 1) \leq (1 - \alpha_j / \bar{\lambda}_P) V_j(t)$. By utilizing (35), we let $c_j = \sqrt{\lambda_P / \bar{\lambda}_P}$ and $\bar{\alpha}_j = \sqrt{1 - \alpha_j / \bar{\lambda}_P}$, arriving at $\|x_p(t)\| \leq c_j \bar{\alpha}_j^{t-t_s-1} \|x_p(t_s + 1)\|$ for $t \in [t_s + 2, t_{s+1}]$.

Furthermore, observing from statement s2) in Theorem 3.1 that $\|x_p(t_s + 1)\| \leq (\|A_j\| + \kappa \|B_{\text{tr}}\|) \|x_p(t_s)\|$ holds for $s \in \mathbb{N}_+$. Noting for $t = t_0 = 0$, since $u_o(0)$ is

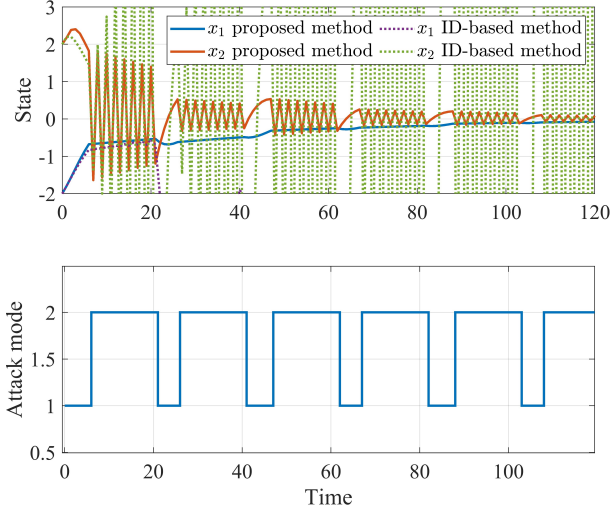


Fig. 3. System performance for Section 4.1. Top: System trajectories under the proposed resilient controller and the ID-based method in Wu et al. (2021); Bottom: Switching times of attacks.

bounded, there exists a constant C_0 such that $\|x(1)\| \leq C_0\|x(0)\|$. Therefore, by defining $C_2 := \max\{C_0, C_1\}$ with $C_1 := \max_{j \in \mathcal{M}} \|A_j\| + \kappa\|B_{\text{tr}}\|$, we have $\|x_p(t_s + 1)\| \leq C_2\|x_p(t_s)\|$ for $s \in \mathbb{N}$.

Let $\hat{c} := \max_{j \in \mathcal{M}} c_j$ and $\hat{\alpha} := \max_{j \in \mathcal{M}} \bar{\alpha}_j$. Combining above results yields for any $t \in [t_s + 1, t_{s+1}]$ that $\|x_p(t)\| \leq C_2 c_j \bar{\alpha}_j^{t-t_s-1} \|x_p(t_s)\| \leq C_2 \hat{c} / \hat{\alpha}^{t-t_s} \|x_p(t_s)\|$. Through telescoping on t and recursively expanding on s , it follows for all $t \in \mathbb{N}$ that

$$\|x_p(t)\| \leq \left(\frac{C_2 \hat{c}}{\hat{\alpha}}\right)^{s+1} \hat{\alpha}^{t-t_0} \|x_p(t_0)\| \quad (36)$$

$$\leq \underbrace{\left(\frac{C_2 \hat{c}}{\hat{\alpha}}\right)^v}_{:=C_3} \left[\left(\frac{C_2 \hat{c}}{\hat{\alpha}}\right)^{\frac{1}{\tau}} \hat{\alpha}\right]^{t-t_0} \|x_p(t_0)\| \quad (37)$$

where the second inequality comes from Assumption 2.4 with $s + 1 = N_\sigma(t_0, t) \leq v + (t - t_0)/\tau$ for some $v \geq 0$. Hence, when $\tau > \bar{\tau}$ with $\bar{\tau} := (\ln \hat{\alpha} - \ln C_2 - \ln \hat{c}) / \ln \hat{\alpha}$ then $0 < (C_2 \hat{c} / \hat{\alpha})^{1/\tau} \hat{\alpha} < 1$. Consequently, upon defining $\beta := (C_2 \hat{c} / \hat{\alpha})^{1/\tau} \hat{\alpha}$, we arrive at $\|x_p(t)\| \leq C_3 \beta^t \|x_p(0)\|$ with the constant C_3 in (37). This completes the proof.

4 Numerical Examples

In this section, we compare the proposed scheme with the system identification-based approach in Wu et al. (2021) and the data-driven method in Rotulo et al. (2022) through two numerical examples. The following simulations were run on a Lenovo laptop with a 14-core 2.3GHz i7-12700H processor.

4.1 Power Generator

Taking the sampling time to be $T_s = 0.1s$, we consider a discretized version of the linearized model of the nor-

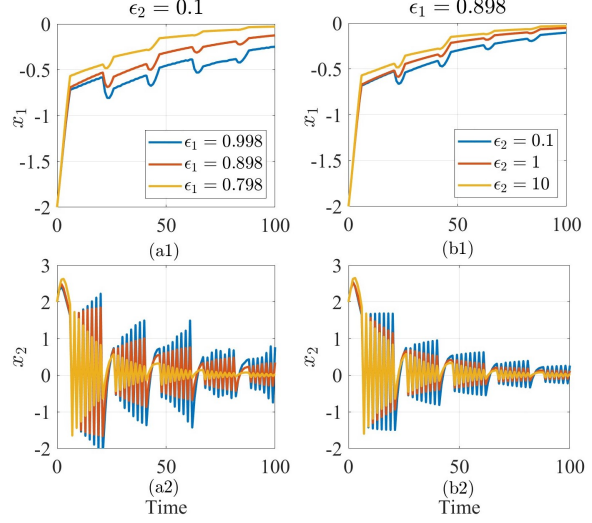


Fig. 4. System's performances under different ϵ_1 and ϵ_2 .

malized swing equation in Wu et al. (2021), where

$$A_{\text{tr}} = \begin{bmatrix} 0 & 1 \\ -1 & -1 \end{bmatrix}, B_{\text{tr}} = \begin{bmatrix} 0 & 0 \\ 1 & 1 \end{bmatrix}, K = \begin{bmatrix} -1 & 0 \\ 0 & -2 \end{bmatrix}. \quad (38)$$

For simplicity, we assume that the attacker knows the matrices $A_{\text{tr}}, B_{\text{tr}}, K$, and generates the attacking matrices using the method in Wu et al. (2021). For a fair comparison, we multiply the obtained attack matrices by 1.2 (i.e., increasing the power of attacks), yielding at-

tacking matrices $B_{\text{tr}} D_a^1 K_a^1 = \begin{bmatrix} -0.0232 & -0.0103 \\ -0.4567 & -0.2025 \end{bmatrix}$ and

$B_{\text{tr}} D_a^2 K_a^2 = \begin{bmatrix} -0.0107 & -0.0929 \\ -0.2110 & -1.8266 \end{bmatrix}$. It is easy to verify that

$\|B_{\text{tr}} D_a^j K_a^j\| \leq 1.841$ for $j = 1, 2$. The switching signal σ is given in the bottom panel of Fig. 3. The resilient controller designed based on a least-squares system identification (ID) method in Wu et al. (2021) is given by

$$u_o(t) = K_{ID} x_p(t) \text{ with } K_{ID} = \begin{bmatrix} 1.6516 & 0.2865 \\ -0.0997 & 1.9777 \end{bmatrix}.$$

Setting $T = 15$, we collect an offline input-state trajectory by applying a sequence of inputs $u(t)$ uniformly generated from $[-0.3, 0.3]$ to the healthy system $(A_{\text{tr}}, B_{\text{tr}})$. Taking $\delta = 0.125$, $\epsilon_1 = 0.898$, and $\epsilon_2 = 1$, over a simulation horizon of 120 time steps, the top panel of Fig. 3 compares the system's performance under the proposed method in Alg. 1 (solid line) and the ID-based resilient controller in Wu et al. (2021) (+ marked dashed line), showcasing the effectiveness of the proposed method. Moreover, the system's performance under different ϵ_1 and ϵ_2 values in SDP (16) is depicted in Fig. 4. It is shown that smaller ϵ_1 and larger ϵ_2 lead to better system's performance. However, when $\epsilon_1 \leq 0.75$, SDP (16) becomes infeasible for some t .

4.2 Aircraft Engine System

In the second example, we consider our approach to stabilizing fault tolerant systems. Specifically, we apply the proposed controller to an F-404 aircraft engine system subject to system fault, see e.g., [Rotulo et al. \(2022\)](#). We consider a discretized linearized version of the system with a sampling period of 0.1 s, and the system matrices are given by

$$A_{\text{tr}} = \begin{bmatrix} 0.867 & 0 & 0.202 \\ 0.015 & 0.961 & -0.032 \\ 0.026 & 0 & 0.803 \end{bmatrix}, \quad B_{\text{tr}} = \begin{bmatrix} 0.011 & 0 \\ 0.014 & -0.039 \\ 0.009 & 0 \end{bmatrix}.$$

Similarly to the previous section, we collect an input-state trajectory of length $T = 21$ by stimulating the system such that $\text{rank}(W_0) = n_x + n_u$ holds. We then run the system online, where unknown faults are characterized by changes in the system matrix A_{tr} , resulting in $\tilde{A} = A_{\text{tr}} + \omega(\sigma(t))D$ with

$$D = \begin{bmatrix} 0.075 & 0 & 0 \\ 0.5 & 1 & 0 \\ 0 & 0 & -0.75 \end{bmatrix}, \quad \omega(\sigma(t)) = \begin{cases} 0.7, & \sigma(t) = 1 \\ 0.6, & \sigma(t) = 2 \\ -0.5, & \sigma(t) = 3 \end{cases}$$

where $\|\omega(\sigma(t))D\| \leq 0.783$. The switching signal $\sigma(t)$ is depicted in Fig 5(d). Letting $\delta = 0.14$, $\epsilon_1 = 0.998$, and $\epsilon_2 = 1$, under the fault switching signal presented in Fig. 5(d), system trajectories under the proposed Alg. 1 (+ marked dotted line), the data-driven method in [Rotulo et al. \(2022\)](#) (solid line), and a time-invariant feedback gain (dashed line) are depicted in Fig. 5(a)–(c), which further corroborates the effectiveness of the proposed method. The system’s performance under different ϵ_1 and ϵ_2 values is depicted in Fig. 6. The average computation time per iteration for the ID-based method in [Wu et al. \(2021\)](#), the method in [Rotulo et al. \(2022\)](#), and the proposed method are 10^{-4} s, 0.3394s and 0.6133s, respectively. Furthermore, by consolidating the SDPs (13) and (16) into single SDP, the computational time decreases to 0.2201s, verifying Remark 3.2.

5 Conclusions

This paper has investigated the stabilization problem of unknown linear systems under FDI attacks on the actuator channels using input-state data. A general FDI attack model was proposed by constraining the switching frequency and the attack power. Based on the model, the FDI-corrupted system can be modeled as a linear switched system. A method for minimally representing the system was developed, by combining online observations from the attacked system with offline data from the healthy system to compute a minimum-volume matrix ellipsoid by solving an SDP. In reminiscent of data-driven LQR, a data-based SDP was formulated and solved, from which a data-driven controller was devised. Both SDPs’ feasibility and exponential stability were

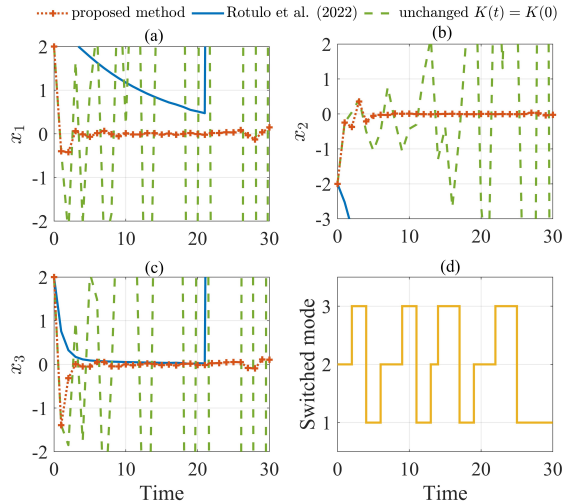


Fig. 5. System’s performance for Section 4.2. Panels (a)–(c): state trajectories under the proposed Alg. 1 (+ marked dotted line), data-driven method in [Rotulo et al. \(2022\)](#) (solid line), and time-invariant controller (dashed line); Panel (d): Switching times.

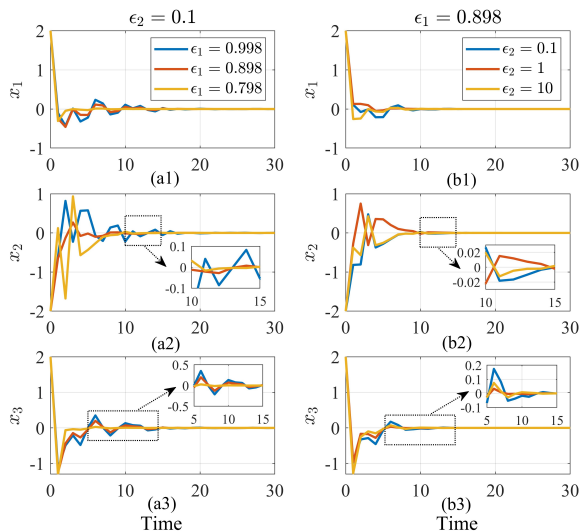


Fig. 6. System’s performances under different ϵ_1 and ϵ_2 .

established Numerical examples were provided to illustrate the efficacy of the proposed controller.

References

- S. C. Anand and A. M. H. Teixeira. Risk-averse controller design against data injection attacks on actuators for uncertain control systems. In *Proc. Amer. Control Conf.*, pages 5037–5042, Atlanta, GA, USA, June, 8-10, 2022.
- C. Bai, F. Pasqualetti, and V. Gupta. Data-injection attacks in stochastic control systems: Detectability and performance tradeoffs. *Automatica*, 82:251–260, Aug. 2017.
- A. Bisoffi, C. De Persis, and P. Tesi. Data-driven control

- via Petersen's lemma. *Automatica*, 145:110537, Nov. 2022.
- A. Cárdenas, S. Amin, and S. Sastry. Secure control: Towards survivable cyber-physical systems. In *Proc. Int. Conf. Distrib. Comput. Syst. Wksp.*, pages 495–500, Beijing, China, June, 16–20, 2008.
- P. Cheng, Z. Yang, J. Chen, Y. Qi, and L. Shi. An event-based stealthy attack on remote state estimation. *IEEE Trans. Autom. Control*, 65(10):4348–4355, Oct. 2019.
- J. Coulson, J. Lygeros, and F. Dörfler. Data-enabled predictive control: In the shallows of the DeePC. In *Proc. Eur. Control Conf.*, pages 307–312, Naples, Italy, June, 25–28, 2019.
- C. De Persis and P. Tesi. Input-to-state stabilizing control under denial-of-service. *IEEE Trans. Autom. Control*, 60(11):2930–2944, Nov. 2015.
- C. De Persis and P. Tesi. Formulas for data-driven control: Stabilization, optimality, and robustness. *IEEE Trans. Autom. Control*, 65(3):909–924, Mar. 2020.
- C. De Persis and P. Tesi. Low-complexity learning of linear quadratic regulators from noisy data. *Automatica*, 128:109548, June, 2021.
- H. Fawzi, P. Tabuada, and S. Diggavi. Secure estimation and control for cyber-physical systems under adversarial attacks. *IEEE Trans. Autom. Control*, 59(6):1454–1467, Jan. 2014.
- S. Feng and P. Tesi. Resilient control under denial-of-service: Robust design. *Automatica*, 79:42–51, 2017.
- N. Hashemi and J. Ruths. Co-design for resilience and performance. *IEEE Trans. Control Netw. Syst.*, Dec. 2022. doi: 10.1109/TCNS.2022.3229774.
- F. Hou, J. Sun, Q. Yang, and Z. Pang. Deep reinforcement learning for optimal denial-of-service attacks scheduling. *Sci. China Inf. Sci.*, 65(6):162201, June, 2022.
- Shubo Kang and Keyou You. Minimum input design for direct data-driven property identification of unknown linear systems. *Automatica*, 156:111130, 2023.
- A. Kotidis and S. Schreft. Cyberattacks and financial stability: Evidence from a natural experiment, 2022. URL <http://dx.doi.org/10.17016/FEDS.2022.025>.
- V. Krishnan and F. Pasqualetti. Data-driven attack detection for linear systems. *IEEE Control Syst. Lett.*, 5(2):671–676, June, 2021.
- E. A. Lee. Cyber physical systems: Design challenges. In *Proc. IEEE Int. Symp. Object Compon.-Oriented Real-Time Distrib. Comput.*, pages 363–369, Orlando, FL, USA, May, 5–7, 2008.
- Y. Li, X. Wang, J. Sun, G. Wang, and J. Chen. Data-driven consensus control of fully distributed event-triggered multi-agent systems. *Sci. China Inf. Sci.*, 66(5):152202, May, 2023.
- W. Liu, J. Sun, G. Wang, F. Bullo, and J. Chen. Data-driven resilient predictive control under denial-of-service. *IEEE Trans. Autom. Control*, 68(8):4722–4737, Aug. 2023a.
- W. Liu, J. Sun, G. Wang, F. Bullo, and J. Chen. Learning robust data-based LQG controllers from noisy data. *IEEE Trans. Autom. Control*, pages 1–13, May, 2023b. doi: 10.1109/TAC.2024.3409749.
- X. Luo, C. Zhao, and J. He. Secure multi-dimensional consensus algorithm against malicious attacks. *Automatica*, 157:111224, Nov. 2023.
- R. McMillan. Ransomware attack affecting likely thousands of targets drags on. <https://www.wsj.com/articles/ransomware-group-behind-meat-supply-attack-threatens-hundreds-of-new-targets-11625285071>, 2021.
- Y. Mo, J. P. Hespanha, and B. Sinopoli. Resilient detection in the presence of integrity attacks. *IEEE Trans. Signal Process.*, 62(1):31–43, Oct. 2013.
- C. Murguia, I. Shames, J. Ruths, and D. Nešić. Security metrics and synthesis of secure control systems. *Automatica*, 115:108757, May, 2020.
- F. Pasqualetti, F. Dörfler, and F. Bullo. Attack detection and identification in cyber-physical systems. *IEEE Trans. Autom. Control*, 58(11):2715–2729, June, 2013.
- M. Rotulo, C. De Persis, and P. Tesi. Online learning of data-driven controllers for unknown switched linear systems. *Automatica*, 145:110519, Nov. 2022.
- M. Shi, S. Feng, and H. Ishii. Quantized state feedback stabilization of nonlinear systems under denial-of-service. *Automatica*, 139:110180, May, 2022.
- Mario Sznaiier. Control oriented learning in the era of big data. *IEEE Control Syst. Lett.*, 5(6):1855–1867, 2020.
- H. J. van Waarde and M. K. Camlibel. A matrix Finsler's lemma with applications to data-driven control. In *Proc. IEEE Conf. Decis. Control*, pages 5777–5782, Austin, TX, USA, Dec. 14–17, 2021.
- M. Wakaiki, A. Cetinkaya, and H. Ishii. Stabilization of networked control systems under DoS attacks and output quantization. *IEEE Trans. Autom. Control*, 65(8):3560–3575, Oct. 2019.
- J. C. Willems, I. Markovskiy, P. Rapisarda, and B. L. M. De Moor. A note on persistency of excitation. *Syst. Control Lett.*, 56(4):325–329, May, 2005.
- G. Wu, G. Wang, J. Sun, and J. Chen. Optimal partial feedback attacks in cyber-physical power systems. *IEEE Trans. Autom. Control*, 65(9):3919–3926, Mar. 2020.
- G. Wu, J. Sun, and L. Xiong. Optimal switching attacks and countermeasures in cyber-physical systems. *IEEE Trans. Syst. Man Cybern. Syst.*, 51(8):4825–4835, Aug. 2021.